

The Impact of Rapid Thermal Annealing on ALCVD- $\text{Al}_2\text{O}_3/\text{Si}_3\text{N}_4/\text{Si}(100)$ Stack Structures -Photoelectron Spectroscopy

F. Takeno¹, A. Ohta¹, S. Miyazaki¹,
K. Komeda², M. Horikawa² and K. Koyama²

¹Grad. School of AdSM., Hiroshima Univ.

²T&D Office, APD Gr., Elpida Memory Inc.

e-mail: semicon@hiroshima-u.ac.jp

ABSTRACT

We studied chemical bonding features and electronic defect states of dielectric stack structures consisting of 5nm-thick Al_2O_3 and 1.7nm-thick Si_3N_4 on Si(100) before and after rapid thermal anneal (RTA) in the temperature range of 850~1000°C for 1min in N_2 or O_2 ambience using X-ray photoelectron spectroscopy (XPS) and total photoelectron yield spectroscopy (PYS). The compositional intermixing at the $\text{Al}_2\text{O}_3/\text{Si}_3\text{N}_4$ interface becomes significant with RTA higher than 900°C. For samples after RTA higher than 950°C in both N_2 and O_2 , Si and N atoms are incorporated throughout the Al_2O_3 layer and detected even on the Al_2O_3 surface. It was noted that the N content in the dielectric layer after O_2 -RTA is smaller than that after N_2 -RTA. This result implies the reaction of diffused N atoms with oxygen and resultant N desorption from the dielectric layer. From PYS measurements, it is found that in the energy region shallower than Si midgap and above, the defect state density of the dielectric after 950°C O_2 -RTA becomes higher by a factor of 2~3 than the case after 950°C N_2 RTA, which might be correlated to the N desorption.

Key words: DRAM, $\text{Al}_2\text{O}_3/\text{Si}_3\text{N}_4$, XPS, PYS

1. INTRODUCTION

Continuous scaling of dynamic random-access memory (DRAM) storage capacitors with shrinking cell area has required the use of a thinner dielectric with a higher dielectric constant (high-k) to maintain charge storage level and charge retention being below some limit on the leakage. In this regard, many studies on high-k dielectrics such as Ta_2O_5 with a dielectric constant of ~25 were performed [1] and, currently, Ta_2O_5 films are widely used for DRAM capacitor dielectrics. However, from the viewpoints of thermal stability and potential barrier height, Al_2O_3 -based films are attracting much attention as the next capacitor dielectrics for further shrinkage of capacitor cells [2]. One of the major difficulties in the scaling of Ta_2O_5 -based capacitor cells is the thickness reduction of an interfacial barrier layer compensating a low potential barrier height of Ta_2O_5 . Because the interfacial layer has a dielectric constant much lower than Ta_2O_5 , the reduction of the total equivalent dielectric thickness is significantly limited by the interfacial layer thickness. Also, thermal and chemical stabilities of Ta_2O_5 against crystallization and interfacial reactions remain a significant barrier to fabricate highly reliable memory cells with a good performance in high temperature processes for transistors. On the other hand, Al_2O_3 is showing promise to overcome such drawbacks of Ta_2O_5 -based dielectrics because of its excellent thermal

stability with silicon, high crystallization over 900°C [3], and favorable potential barrier height higher than 2eV for both electrons and holes [4, 5]. In fact, a good electrical performance of trench capacitors with an Al_2O_3 layer formed by an atomic-layer chemical vapor deposition (ALCVD) has been reported [6, 7]. For the practical implementation of Al_2O_3 to DRAM capacitors, one major concern is how to minimize interfacial reactions between Al_2O_3 and a base material during CVD and post-deposition annealing at high temperature [8]. Thus, a clear insight into the interfacial reactions is definitely needed for better control of interface and film properties.

In this work, we focused on $\text{Al}_2\text{O}_3/\text{Si}_3\text{N}_4$ stack structures formed on Si(100) and evaluated changes in chemical bonding features and electronic defect states in the dielectric stack with rapid thermal annealing (RTA) in N_2 or O_2 ambience.

2. EXPERIMENTAL

After standard chemical cleaning steps of 300mm p-type Si(100) wafers with a resistivity of 8~12 Ω ·cm, the Si(100) wafer surface was nitrided in NH_3 ambience at a temperature of 1100°C to form a uniform ~1.7nm-thick Si_3N_4 layer. Subsequently, a ~5.0nm-thick Al_2O_3 layer was grown on the Si_3N_4 layer by an ALCVD technique at a temperature of 450°C, where trimethyl-aluminum ($\text{Al}(\text{CH}_3)_3$) and O_3 were used as precursors. The $\text{Al}_2\text{O}_3/\text{Si}_3\text{N}_4/\text{Si}(100)$ stack

structures so prepared were annealed in the temperature range of 850–1000°C for 1min in pure N_2 (N_2 -RTA) or dry O_2 (O_2 -RTA). The compositional profiles and chemical bonding features of the samples were examined by x-ray photoelectron spectroscopy (XPS) using monochromatized AlK_α (1486.7eV) radiation in combination with wet-chemical thinning of the dielectric layers in a dilute HF solution. The defect state densities in the stack structures were measured by total photoelectron yield spectroscopy (PYS) [9].

3. RESULTS AND DISCUSSION

The $\text{Si}2p$ spectra taken after N_2 - and O_2 -RTA at 1000°C are compared with the $\text{Si}2p$ spectrum taken before RTA in Fig. 1. For the $\text{Si}2p$ signals due to Si-N bonds peaked around ~102eV, the signal intensity of the higher binding energy side is markedly increased by the N_2 - and O_2 -RTA. This result indicates the formation of Si-O bonds. It is interesting to note that in the sample after the N_2 -RTA, the chemically shifted $\text{Si}2p$ peak appears at higher binding energy by ~0.2eV than the peak after the O_2 -RTA. Since a similar energy shift is observed for the $\text{Al}2p$, $\text{O}1s$ and $\text{N}1s$ spectra as shown in Fig. 2, it is likely that the N_2 -RTA causes the generation of positive charges in the stack structure or the annihilation or neutralization of negative charges possibly existing in the as-deposited Al_2O_3 layer. In addition, the $\text{N}1s$ signal intensity normalized by the $\text{Si}2p$ intensity for the sample after the O_2 -RTA is small compared with that after the N_2 -RTA, in contrast to intense $\text{O}1s$ and $\text{Al}2p$ signals. This result implies the desorption of N atoms by the O_2 -RTA.

Figure 3 shows the changes in $\text{Al}2p$, $\text{Si}2p$ and $\text{N}1s$ spectra for the sample after N_2 -RTA at 1000°C with progressive HF-etching steps. The chemically shifted $\text{Si}2p$ and $\text{N}1s$ signals from the dielectric stack are decreased with progressive thinning of the Al_2O_3 layer. This suggests that Si and N atoms in the Si_3N_4 layer formed at 1100°C are diffused and incorporated into the Al_2O_3 layer. Also, considering the fact that in the early stages of Al_2O_3 thinning (within 30s in etch time), slight decreases in the chemically shifted $\text{Si}2p$ and $\text{N}1s$ signals

are observable, indicating that some Si and N atoms are diffused close to the surface. In Fig. 4, for the samples before and after N_2 - and O_2 -RTA at different temperatures, the integrated intensities of chemically shifted $\text{Si}2p$ and $\text{N}1s$ signals are plotted as a function of the integrated intensity of $\text{Al}2p$ signals, where all these signals were normalized by the $\text{Si}2p$ signal intensity from $\text{Si}(100)$. The results obtained for the cases of 1000°C and 950°C RTA are very similar and irrespective of annealing ambience. Even in the early stages of wet-chemical etching, $\text{Si}2p$ and $\text{N}1s$ signals are decreased with a reduction in the $\text{Al}2p$ signals and disappear slightly earlier than $\text{Al}2p$ signals. This indicates that thin Si_3N_4 layer can not survive by RTA over 950°C and Si and N atoms diffuse near the surface, that is, almost complete compositional intermixing occurs in the stack structure. In contrast, for the case after 850°C RTA, the $\text{Si}2p$ signals are reduced only by 20% from the initial intensity when no $\text{Al}2p$ signal is detectable, suggesting that the Si_3N_4 layer remains after the RTA although some Si atoms diffuse into the Al_2O_3

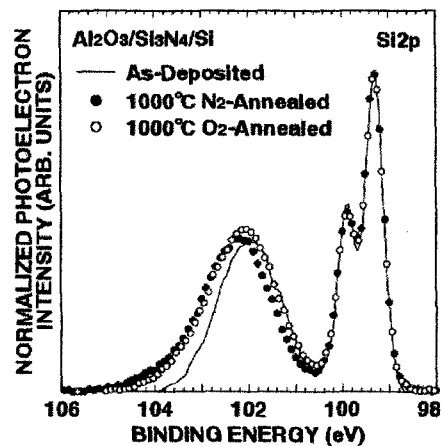


Fig. 1. $\text{Si}2p$ spectra for as-prepared $\text{Al}_2\text{O}_3(5.0\text{nm})/\text{Si}_3\text{N}_4(1.7\text{nm})/\text{Si}(100)$ (solid line) and after being annealed in N_2 ambience (closed dots) and in O_2 ambience (open dots) at 1000°C. The photoelectron take-off angle was set at 90°.

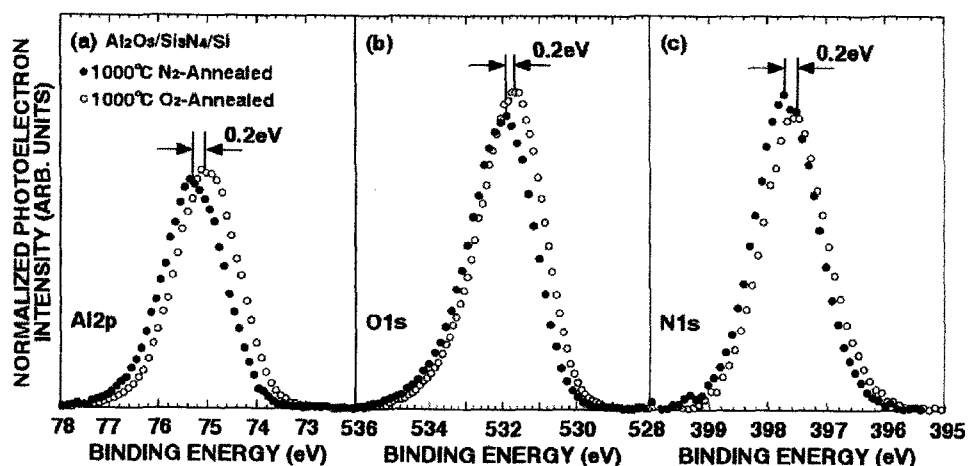


Fig. 2. $\text{Al}2p$ (a), $\text{O}1s$ (b) and $\text{N}1s$ (c) spectra for $\text{Al}_2\text{O}_3(5.0\text{nm})/\text{Si}_3\text{N}_4(1.7\text{nm})/\text{Si}(100)$ after being annealed in N_2 ambience (closed dots) and in O_2 ambience (open dots) at 1000°C. The binding energy was calibrated by the $\text{Si}2p_{3/2}$ peak at 99.3eV for the $\text{Si}(100)$ substrate and the photoelectron intensity was normalized by the peak intensity of $\text{Si}2p$ signals from the $\text{Si}(100)$ substrate.

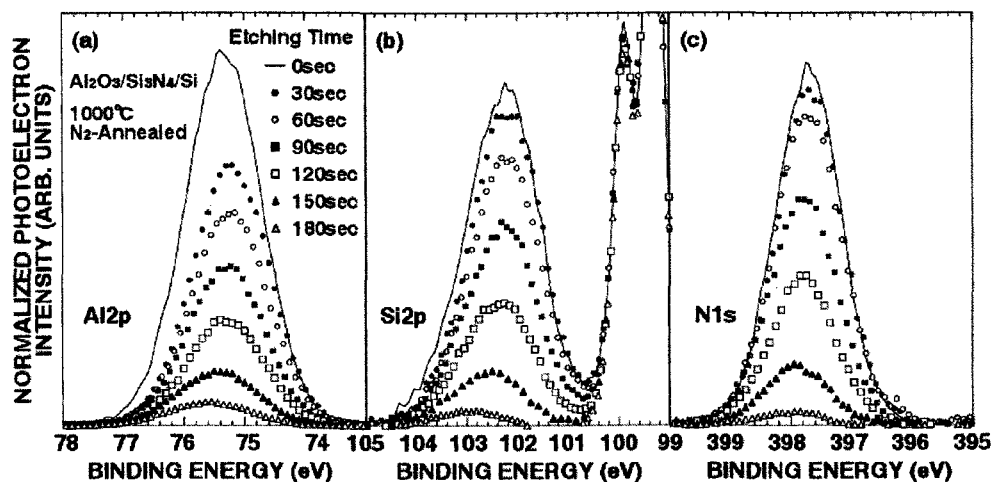


Fig. 3. Al2p (a), Si2p (b) and N1s (c) spectra taken at each thinning step of the dielectric stack in a diluted HF solution for the sample annealed in N₂ ambience at 1000°C. The binding energy was calibrated by the Si2p_{3/2} peak at 99.3eV for the Si(100) substrate and the photoelectron intensity was normalized by the peak intensity of Si2p signals from the Si(100) substrate.

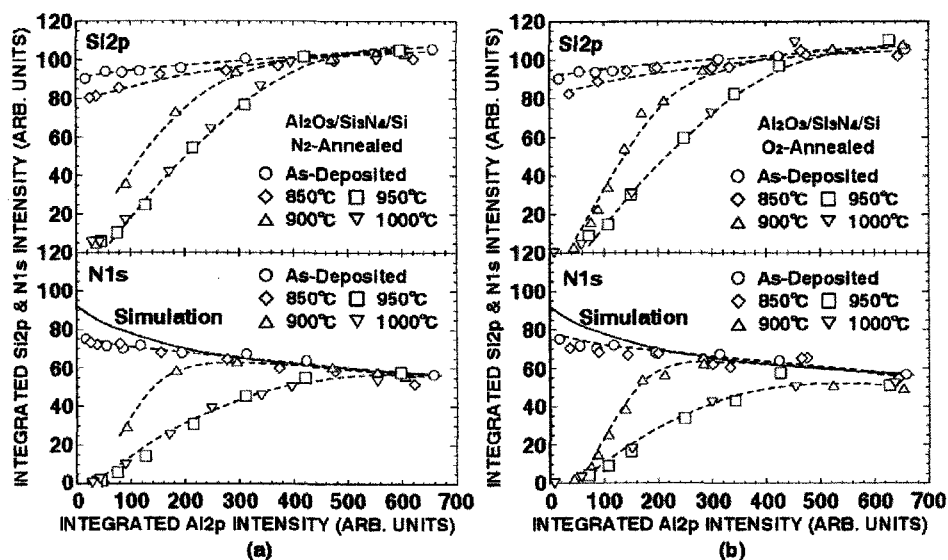


Fig. 4. Integrated intensities of chemically shifted Si2p and N1s signals as a function of integrated Al2p signal intensity for as-deposited Al₂O₃/Si₃N₄/Si and annealed in N₂ (a) and O₂ (b) ambience at different temperatures.

layer. Also, since the N1s intensity becomes markedly smaller than the simulated result for the case of ideal Al₂O₃/Si₃N₄ stack as the Al₂O₃ thinning proceeds close to the interfacial region, it is likely that a compositional mixing between Al₂O₃ and Si₃N₄ occurred in an atomic layer scale. Considering there was no difference in N1s intensity between the cases before and after the 850°C RTA, the interfacial reaction in the early stages of Al₂O₃ ALCVD on Si₃N₄ might be responsible for such a slight intermixing. In the simulation, an increase in the N1s intensity with decreasing Al2p intensity is attributed to the fact that the escape depth of the N1s photoelectrons in the Al₂O₃ film is smaller than that of the Si2p photoelectrons by a factor of 0.83. It is also found that there is no significant difference between the results obtained after N₂- and O₂-RTA except that O₂-RTA at 950 and 1000°C causes a slight reduction of N atoms in the dielectric stack.

To examine the influence of the composition

intermixing gives on the electronic defect state density in the stack structures, photoelectron yields from the samples before and after RTA were measured as a function of incident photon energy as shown in Fig. 5. For incident photons with energies higher than ~5.2eV, the electron emission from the Si valence band becomes significant as indicated in the region colored in gray. By Al₂O₃ ALCVD on Si₃N₄/Si(100), the photoelectron yield in the energy region below ~5.2eV is remarkably increased, which implies existence of filled defect states in the Al₂O₃ layer and/or defect generation at the interface between Al₂O₃ and Si₃N₄. No significant change in the yield is caused by RTA at 850°C. When the RTA temperature rises up to 950°C, the photoelectron yield is decreased by more than one order of magnitude; namely, the filled defect states in the as-prepared Al₂O₃/Si₃N₄ stack structure are reduced well. Note that the photoelectron yield after O₂-RTA at 950°C is 2~3 times higher than that of N₂-RTA (Fig. 5(b)).

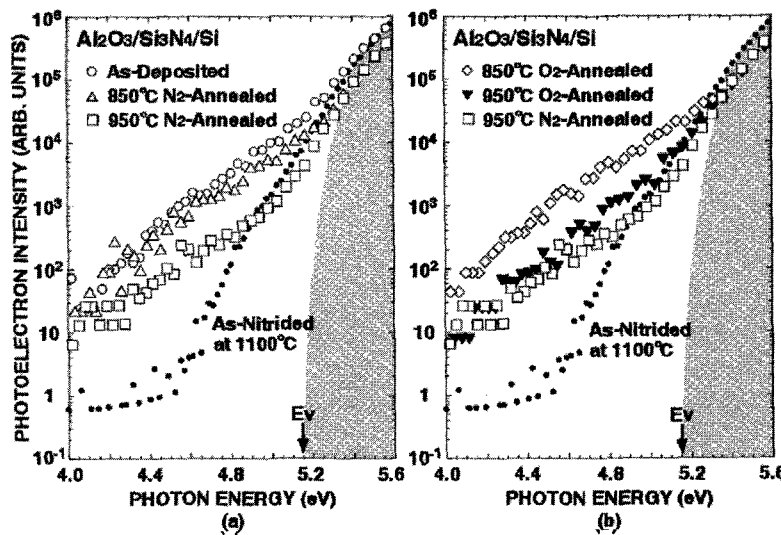


Fig. 5. Total photoelectron yield spectra for as-prepared $\text{Al}_2\text{O}_3(5.0\text{nm})/\text{Si}_3\text{N}_4(1.7\text{nm})/\text{p-Si}(100)$ and after annealed in N_2 ambience (a) and comparison with the yield spectra for the cases annealed in O_2 ambience. The yield spectrum of as-nitrided $\text{Si}(100)$ is also shown as a reference. E_v denotes the Si valence band top measured from the vacuum level.

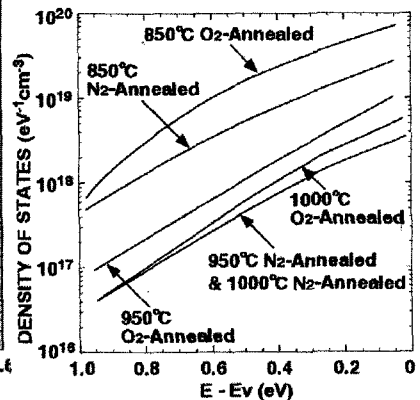


Fig. 6. Energy distributions of the density of occupied defect states for the samples shown in Fig. 5 and for the samples annealed at 1000°C . The vertical scale is expressed in volume density.

Such a tendency of a higher yield being obtained by O_2 -RTA than N_2 -RTA, is also found in the cases at 850°C and 900°C RTA. Based on the result obtained by XPS measurements (see Fig. 4), the desorption of N atoms from the dielectric stack caused by O_2 -RTA is likely to impede the defect annihilation in the dielectric stack structure or may create vacancies acting as electronic defects. From the first derivative of the PYS spectra with respect to photon energy, we crudely estimated the defect state density in the dielectric stack structure, where the density of state in the Si valence band and the photoelectron escape depth were taken into account. Details on converting the measured PYS spectrum to the energy distribution of filled defect states are described in Ref. 9. The filled defect state density in as-deposited and O_2 -RTA at 850°C is of the order of $10^{19} \text{ eV}^{-1} \text{ cm}^{-3}$ at an energy near the Si midgap, and by N_2 -RTA at 950°C and higher, it is decreased efficiently and to $\sim 3 \times 10^{17} \text{ eV}^{-1} \text{ cm}^{-3}$ at an energy near the Si midgap.

4. CONCLUSIONS

We have studied chemical bonding features and defect densities of $\text{Al}_2\text{O}_3/\text{Si}_3\text{N}_4/\text{Si}(100)$ stack structures before and after annealing in the temperature range of $850\text{--}1000^\circ\text{C}$ in N_2 and O_2 ambience using photoelectron spectroscopy. In the RTA process higher than 900°C , Si and N atoms in the ultrathin Si_3N_4 layer formed in NH_3 gas ambience at 1100°C diffuse significantly into the Al_2O_3 layer. The RTA at 900°C or higher is very effective in decreasing the defect density in the stack structures. The residual filled defect density in RTA in the O_2 ambience tends to be higher than that in N_2 ambience. The N desorption from the dielectric layer resulting from the reaction of diffused N atoms in the Al_2O_3 layer with oxygen may involve higher residual defects in O_2 -RTA than in N_2 -RTA.

REFERENCES

- [1] N. Nishioka, *Mat Res. Soc. Symp. Proc.* 567 (1999) 361.
- [2] S. Jakschik, U. Schroeder, T. Hecht, A. Berbmaier and J. W. Bartha, *Mat. Sci. and Eng B107* (2004) 251.
- [3] S. Jakschik, U. Schroeder, T. Hecht, M. Gutsche, H. Seidl and J. W. Bartha, *Thin Solid Films* 425 (2003) 216.
- [4] J. Robertson, *J. Vac. Sci. Technol. B18* (2000) 1785.
- [5] S. Miyazaki, *J. Vac. Sci. Technol. B19* (2001) 2212.
- [6] M. Gutsche, H. Sedl, J. Luetzen, A. Birner, T. Hecht, S. Jaschik, M. Kerber, M. Leonhardt, P. Moll, T. Pompl, H. Reisinger, S. Rongen, A. Saenger, U. Schroeder, B. Sell, A. Wahl and D. Schumannet, *Tech. Dig. IEEE Int. Electron Device Meeting*. (2001, Washington) p. 411.
- [7] H. Seidl, M. Gutsche, U. Schroeder, A. Birner, T. Hecht, S. Jaschik, J. Luetzen, M. Kerber, S. Kudelka, T. Topp, A. Orth, H. Reisinger, A. Saenger, K. Schupke and B. Sell, *Tech. Dig. IEEE Int. Electron Device Meeting*. (2002, San Francisco) p. 839.
- [8] H. Bender, T. Conard, H. Nohira, J. Pertry, C. Zhao, B. Brijs, W. Besling, C. Detavernier, W. Vandervorst, M. Caymax, S. De Gendt, J. Chen, J. Kluth, W. Tsai and J. W. Maes, *Proc. of Int. Workshop on Gate Insulators* (2001, Tokyo) p. 86.
- [9] S. Miyazaki, T. Maruyama, A. Kohno and M. Hirose, *Microelectron. Eng.* 48 (1999) 63.

(Received January 10, 2005; Accepted February 3, 2005)